Advanced seismic processing/ imaging techniques and their potential for geothermal exploration

Review Article

Author(s):
Schmelzbach, Cédric; Greenhalgh, Stewart A.; Reiser, Fabienne; Girard, Jean-François; Bretaudeau, François; Capar, Laure; Bitri, Adnand

Publication date:
2016-11

Permanent link:
https://doi.org/10.3929/ethz-b-000188810

Originally published in:
Interpretation 4(4), https://doi.org/10.1190/int-2016-0017.1

Funding acknowledgement:
608553 - Integrated Methods for Advanced Geothermal Exploration (EC)

Advanced seismic processing/imaging techniques and their potential for geothermal exploration

Cédric Schmelzbach[1], Stewart Greenhalgh[1], Fabienne Reiser[1], Jean-François Girard[2], François Bretaudeau[3], Laure Capar[3], and Adnand Bitri[3]

Abstract

Seismic reflection imaging is a geophysical method that provides greater resolution at depth than other methods and is, therefore, the method of choice for hydrocarbon-reservoir exploration. However, seismic imaging has only sparingly been used to explore and monitor geothermal reservoirs. Yet, detailed images of reservoirs are an essential prerequisite to assess the feasibility of geothermal projects and to reduce the risk associated with expensive drilling programs. The vast experience of hydrocarbon seismic imaging has much to offer in illuminating the route toward improved seismic exploration of geothermal reservoirs — but adaptations to the geothermal problem are required. Specialized seismic acquisition and processing techniques with significant potential for the geothermal case are the use of 3D arrays and multicomponent sensors, coupled with sophisticated processing, including seismic attribute analysis, polarization filtering/migration, converted-wave processing, and the analysis of the diffracted wavefield. Furthermore, full-waveform inversion and S-wave splitting investigations potentially provide quantitative estimates of elastic parameters, from which it may be possible to infer critical geothermal properties, such as porosity and temperature.

Introduction

Geothermal energy is a promising and increasingly popular sustainable energy source for electricity generation and district heating purposes (Lund, 2009). However, considerable further research and development is necessary to optimize this renewable energy source in terms of the engineering challenges and the geoscientific requirements to identify, locate, and produce geothermal reservoirs. In many places, the high temperatures needed for economical geothermal electricity production are generally found at depths of at least a few kilometers in the earth's crust. Suitable subsurface imaging tools are required to delineate and characterize geothermal reservoirs in sufficient detail at these depths.

Seismic reflection imaging has a greater depth of penetration with reasonable resolution compared with other geophysical methods used to investigate geothermal reservoirs (e.g., gravity, magnetic, electrical resistivity, and electromagnetic surveys; Barbier, 2002). Seismic reflection investigations map interfaces associated with elastic-property contrasts (i.e., reflecting/scattering features; Sheriff and Geldart, 1995; Yilmaz, 2001) and can provide estimates of physical properties, such as seismic velocities and anisotropy. Potential and diffusive field geophysical techniques such as gravity surveying and electromagnetic imaging provide large-scale subsurface volume information (bulk properties). For example, electromagnetic methods have successfully been used in geothermal exploration to image the subsurface electrical resistivity distribution, which is sensitive to fluid content, temperature, and alteration (Muñoz, 2014). Passive seismic techniques such as ambient noise tomography and microseismicity studies (Obermann et al., 2015) have been successfully used to characterize geothermal reservoirs and to monitor changes. However, it is essentially only active (controlled source) seismic methods that can provide the necessary high-resolution fault and fracture characterization at depth necessary for successful well siting.

Oil companies have explored in great detail many sedimentary basins throughout the world; hence, much can be learned from the oil and gas industry in terms of advanced exploration techniques. For example, fracture zone imaging and characterization is of equal importance to hydrocarbon exploration as it is to geothermal exploration. Key developments in land-seismic acquisition and processing for oil and gas exploration that are relevant to geothermal exploration include

[1]Institute of Geophysics, ETH Zurich, Switzerland. E-mail: cedric.schmelzbach@erdw.ethz.ch; stewart.greenhalgh@erdw.ethz.ch; fabienne.reiser@erdw.ethz.ch.
[2]BRGM, Orléans, France and Institut de Physique du Globe de Strasbourg, Strasbourg, France. E-mail: jf.girard@unistra.fr.
[3]BRGM, Orléans, France. E-mail: f.bretaudeau@brgm.fr; l.capar@brgm.fr; a.bitri@brgm.fr.
Manuscript received by the Editor 29 January 2016; revised manuscript received 18 March 2016; published online 4 August 2016. This paper appears in *Interpretation*, Vol. 4, No. 4 (November 2016); p. SR1–SR18, 9 FIGS.
http://dx.doi.org/10.1190/INT-2016-0017.1.

3D and repeated 3D (4D; time-lapse) technology (Lumley, 2001; Brown, 2004), multicomponent seismic measurements (Hardage et al., 2011), advanced and efficient prestack migration schemes (prestack time and depth migration, reverse time migration; Yilmaz, 2001), seismic attribute and amplitude variation with offset analyses (Luo and Evans, 2004; Chopra and Marfurt, 2007), and anisotropy studies (Crampin, 1985).

Enhanced geothermal systems (EGS) have their maximum potential in crystalline basement rock (Tester et al., 2007) in which temperatures are sufficiently elevated but the permeability is low and in need of artificial stimulation. So far, extensive seismic exploration studies over hard-rock environments (for a comprehensive review, see Eaton 2003) are mainly related to mineral exploration (Milkereit et al., 1994; Drummond et al., 2003; Malehmir et al., 2012), mapping fracture zones primarily for finding suitable underground repositories for radioactive waste (Green and Mair, 1983; Juhlin and Palm, 2003; Schmelzbach et al., 2007), and assorted geologic studies, especially crustal investigations (Clowes et al., 1984; Juhlin et al., 1998; Cook et al., 1999; Schmelzbach et al., 2008a, 2008b).

There are several key challenges one needs to face in hard-rock seismic exploration (Salisbury et al., 2003; Greenhalgh and Manukyan, 2013): (1) reflection amplitudes are generally weak, leading to low signal-to-noise ratio (S/N) that makes it difficult to image features within crystalline rocks; (2) reflectors are often small, steeply dipping, and laterally discontinuous due to more complex morphology, lithology, and deformation; (3) the high velocities in crystalline basement result in a loss of resolution due to the relatively longer wavelengths; (4) obtaining reliable velocity information in deep basement is problematic without long aperture recordings; and (5) anisotropy can be introduced through fractures and layering, leading to complex wave propagation. Milkereit and Eaton (1998) discuss in detail the seismic challenges that occur in crystalline basement in comparison with sedimentary basins. Low-reflection coefficients make it difficult not only to image large scale structures, such as the Moho discontinuity or major fault structures, but also to obtain a detailed shallow crustal image. Deep crustal studies helped to develop the requisite acquisition and processing techniques for crystalline environments, including metalliferous mining. These large-scale images can also provide valuable information when looking for potential geothermal sites. They can be used as a basis for a more refined study of a promising area and further evaluation of the site.

Although it is used extensively in hydrocarbon exploration and production, seismic reflection imaging has been only rarely used in geothermal exploration to date, with a few notable exceptions (e.g., in the Bavarian Molasse Basin and the Upper Rhine Graben in Germany). However, active-source seismic surveying provides a powerful and essential prerequisite to assess the feasibility of geothermal projects and to reduce the risk associated with expensive drilling programs. Moreover, seismic imaging enables more intelligent and selective drilling. Targets in geothermal exploration are permeable zones of sufficiently high temperature and fluid movement; such zones are mostly controlled by faults and fractures. Hence, the focus in seismic geothermal exploration is mapping deep sedimentary and basement structures, such as faults and fracture zones.

Various sophisticated seismic imaging techniques have been developed for the oil and gas industry as well as for the mining industry, not only for exploration but also for monitoring of reservoirs during production. It needs to be investigated how these techniques can be adapted and applied to geothermal sites to improve the planning and development of geothermal reservoirs. In this paper, we (1) summarize the challenges and current status of geothermal seismic exploration, (2) discuss how geothermal seismic exploration can benefit from experience with seismic methods in hydrocarbon and metalliferous-ore exploration, and (3) review a selection of advanced seismic processing techniques that could potentially be of value for the seismic imaging and evaluation of geothermal reservoirs.

Status of geothermal seismic exploration

Permeable fracture zones control the fluid flow in sedimentary and hard-rock geothermal reservoirs and, therefore, need to be considered in the planning of wells. Some examples of seismic reflection investigations in geothermal areas for EGS and hydrothermal systems are described in the following two subsections.

Hydrothermal systems

A geothermal system that contains a naturally occurring permeable layer or layers and a large amount of fluid or vapor that circulates in the subsurface is called a hydrothermal system (Barbier, 2002). Whether the system is economically viable depends on the amount of water or steam that can be extracted and the drilling depth that is necessary to reach the necessary rock temperature. A geothermal reservoir can exist in various depth ranges, depending on surrounding heat sources. High enthalpy systems are mostly related to recent volcanism, show high temperatures at relatively shallow depth and are responsible for most of the electricity production from geothermal areas. Examples for hydrothermal systems in Europe that successfully produce electricity are Lardarello in Italy (Brogi et al., 2005) and several reservoirs in Iceland (Arnórsson, 1995).

However, moderate-temperature geothermal resources can also be used for electricity production. Deep sedimentary basins that contain an aquifer that enables the fluid to circulate, e.g., the porous sandstone in the North German sedimentary basin (Schellschmidt et al., 2010; Weber et al., 2015), or faulted reservoirs, e.g., Unterhaching, near Munich, where large fault systems and karstification provide good hydraulic conductivity (Thomas and Schulz, 2007; Lüschen et al., 2014) can be used for electricity generation.

Because hydrothermal systems are naturally occurring, they are limited in geographic location and it is a key challenge to find them. Seismic exploration can be used to image the lateral extent of an aquifer and to characterize the associated fault and fracture systems (Matsushima and Okubo, 2003). Examples of seismic exploration in hydrothermal systems are the study by von Hartmann et al. (2012) who reprocess a relatively low common-depth-point (CDP) fold (approximately 12) 3D seismic data set acquired in 1985 for hydrocarbon exploration in southern Germany to resolve and characterize Upper Jurassic carbonate platforms that could serve as a geothermal reservoir. Lüschen et al. (2014) study a 3D seismic data set covering an area of approximately 27 km^2 in Unterhaching, Munich, to characterize the Malm sequence that is the target formation for a hydrothermal reservoir (see also Thomas et al., 2010). The 3D data enabled the mapping of key tectonic features in 3D (Figure 1) and the analysis of azimuth-dependent reflectivity to obtain indications of the preferred fracture orientations (Figure 2).

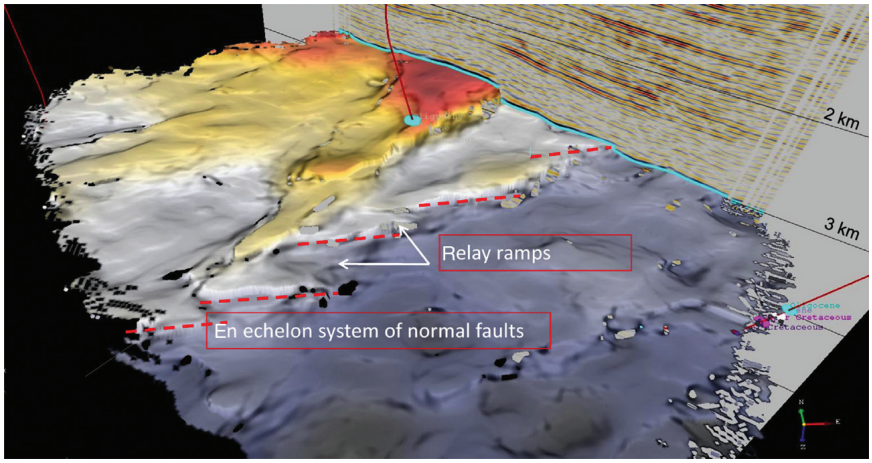

Figure 1. Mapping key lineaments around the Unterhaching (Munich area, Germany) geothermal site using 3D seismic-reflection imaging. The extent of the Lithothamnion limestone horizon is shown at approximately 3000 m depth; colors ranging from red to dark blue represent differences in depth of approximately 500 m. The Unterhaching Gt2 well is shown in red. Background shows a vertical section through the 3D data cube. Figure reprinted from Lüschen et al. (2014), Copyright (2014), with permission from Elsevier.

Pussak et al. (2014) process a 3D seismic data set from the Polish Basin to investigate a lower Jurassic horizon that consists of alternating sandstone and claystone layers. The target geothermal reservoir was imaged using a common-reflection-surface (CRS) stack technique (Jäger et al., 2001) and compared with the results of a conventional normal moveout and dip moveout stack (Yilmaz, 2001). A similar study was conducted by Buness et al. (2014) in the Upper Rhine Graben. It was shown that a CRS stack improved the S/N and is an especially valuable method for sparse data sets because reflections are sampled over several CDP bins instead of just one as in conventional CDP stacking. Amplitude analysis was successfully used to image fault zones.

Deep crustal large-scale seismic images can provide valuable information when looking for potential geothermal sites. An example of imaging the shallow crust for geothermal exploration is given by Brogi et al. (2005) and Riedel et al. (2015). Two deep seismic reflection lines were acquired in southern Tuscany to examine the Lardarello geothermal site. The study helped to understand the tectonic setting, to construct a regional structural model, and to identify a magmatic body that could serve as a current heat source for the Lardarello geothermal site.

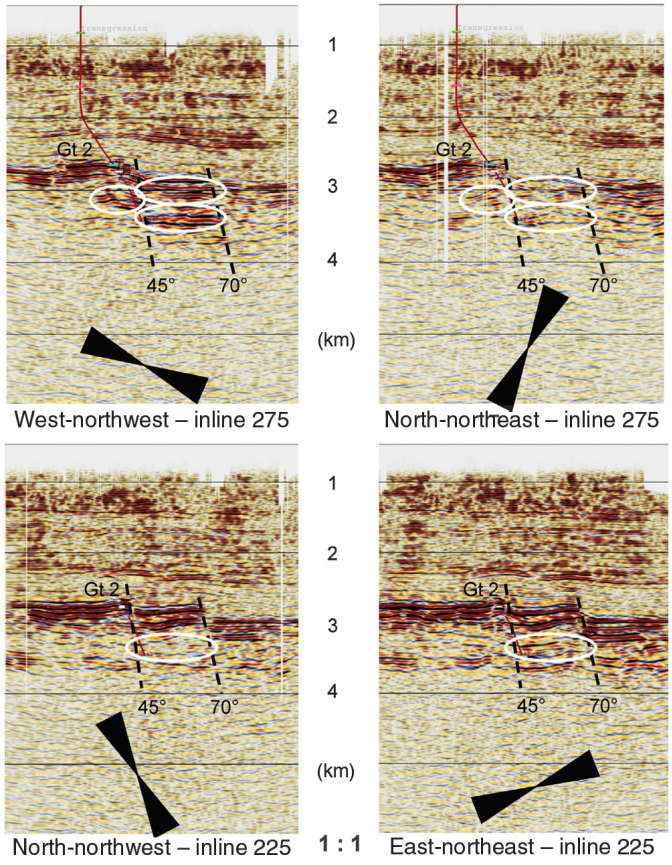

Figure 2. Azimuth selective processing of the Unterhaching 3D seismic data. The four vertical sections show the processed data for 30° wide source-receiver corridors. Width and orientation of the angle corridors are indicated by the black triangles. Amplitudes are plotted at the same scale. The dashed lines mark the main fault zones and white ellipses mark regions with azimuth-dependent reflectivity. Drill trajectory of well Gt2 is shown in red. Figure reprinted from Lüschen et al. (2014), Copyright (2014), with permission from Elsevier.

Enhanced geothermal systems

EGSs have great potential because they are not limited to specialized geologic environments, such as hydrothermal and magmatic systems. EGSs are an

emerging technology, and several research programs have been developed along with pilot plants and the installations have been tested. Examples of EGS can be found worldwide and include Fenton Hill (USA; Duchane and Brown, 2002), Soultz-sous-Forêts (France; Genter et al., 2010; Gérard et al., 2006), Rosemanowes Quarry (UK; Richards et al., 1994), Hijiori and Ogachi (Japan; Kuriyagawa and Tenma, 1999), Cooper Basin (Australia; Chopra and Wyborn, 2003), and The Geysers (USA; Lipman et al., 1978).

EGS can be built in many locations worldwide, where a suitable hot rock volume is accessible in the upper few kilometers of the crust (Lund, 2009). These rocks show very low natural permeability, and, hence, the reservoirs need to be artificially fractured to produce a hydraulically conductive subsurface to circulate fluid. Favorable locations for an EGS show a great amount of heat in place and an insulating sedimentary cover layer to retain the heat. Hence, most EGS reservoirs will be located in hard-rock basement rather than in the sedimentary section.

The emphasis of seismic exploration in EGS areas has been on detailed imaging of fault and fracture zones at the top of and within the crystalline basement. Seismic reflection images reveal the subsurface structure and/or stratigraphy and can therefore be used to help establish flow models and find favorable positions for wells. However, there has only been little research on hard-rock seismic reflection imaging in geothermal areas. A few examples are summarized below.

The Rhine Graben is currently one of the main European areas for EGS projects in predominantly crystalline rocks. Sites of planed, active, or ceased geothermal power plants in the Rhine Graben are Soultz-sous-Forêts (France), Landau (Germany), Insheim (Germany), Rittershoffen (France), and Basel (Switzerland). Place et al. (2010) interpret several reprocessed vintage seismic lines in the Soultz-sous-Forêts geothermal site (see also Sausse et al., 2010; Place et al., 2011). A large number of seismic lines are available due to extensive oil exploration in the area. By focusing on improved static corrections and time migration, some sedimentary reflectors were mapped in greater detail. However, due to the fact that the acquisition parameters (e.g., maximum offset) were originally chosen to image the shallower sediments, the top of the basement and the deeper sediments were not well imaged. Hence, even after reprocessing, structures of geothermal interest within the basement were not recovered.

Recently, Hloušek et al. (2015a) and Schreiter et al. (2015) report on the processing and interpretation, respectively, of a 3D survey of approximate areal extent 10×13 km that was conducted in 2012 in western Erzgebirge near the city of Schneeberg, Germany (see also Ahmed et al., 2015; Lüschen et al., 2015). The aim of the project was to characterize the major fracture zones in the crystalline rock at approximately 4–5 km depth. With expected temperatures of 160–180°, this fracture zone could be used as a natural heat exchanger. An advanced coherency-style prestack depth migration algorithm (Hloušek et al., 2015b) sharpened the image and revealed several fracture zones in 2–5 km depth interval.

Abul Khair et al. (2015) establish a seismic workflow for EGS to characterize faults within deep hot granites. The study site is the Cooper Basin of South Central Australia which is defined by a 3 km thick sediment cover, which serves as a good thermal insulator over a granitic basement. The aim of the project was to image and to identify faults that are most likely to provide the pathways for the circulating fluids.

Vertical seismic profiling at geothermal sites

Vertical seismic profiling (VSP) has been widely used in the oil industry to complement surface seismic data (Hardage, 2000) but its use in geothermal exploration has been somewhat restricted to just checkshot-style surveys for average velocity estimation and converting times to depths. VSPs entail placing receivers downhole and firing into them from surface shots (or other energy sources) at various offsets from the wellhead (including at wellhead, corresponding to zero offset) and different azimuths. VSPs can be applied to identify reflections and trace them to their points of origin in the subsurface, provide information about their orientation and exact location when they intersect the borehole, and tie borehole geology to surface seismic data. They provide the elusive link between synthetic seismograms and actual seismic records. Furthermore, they can be used to image structures away from the well. Because of their many advantages, VSPs can be used for high-resolution imaging of lithologic interfaces and dipping features (e.g., fracture zones) in the vicinity of the borehole. Valuable reflectivity, velocity, and anisotropy information can be gained from VSP data. In addition, it is very beneficial for providing a direct linkage between lithology in the borehole and the seismic data, and obtaining accurate velocity values as a function of depth that can be used for the time-depth conversion of surface seismic data.

Cosma et al. (2003) discuss several advantages of VSP over surface seismic data in crystalline rock:

1) Because receivers are placed within the well, traveltimes are shorter, and waves travel only once through the highly attenuating near-surface weathered layer, hence, the signal amplitudes experience less attenuation than in surface seismic data, resulting in generally superior resolution.
2) To map dipping features with surface seismic reflection data, large offsets are required. VSP provides a convenient geometry for mapping gently and steeply dipping interfaces, especially for multioffset and multiazimuth surveys.
3) 3C geophones enable the recording of the full vector wavefield and with polarization analysis, the orientation of reflectors can be retrieved, whereas in surface seismic data, the polarization information is

often degraded due to the heterogeneous and low-velocity near-surface layer.

VSP surveys have successfully been applied in fractured carbonate reservoirs (Emsley et al., 2007) and in crystalline rock for better understanding of seismic properties in the crust (Carr et al., 1996; Rabbel et al., 2004), for mineral exploration (Adam et al., 2003; Bellefleur et al., 2004), and nuclear waste disposal sites (Cosma et al., 2003).

There have also been a few examples in which VSP has been used to better characterize geothermal sites. Majer et al. (1988) report a VSP pilot study in The Geyser steam-bearing geothermal field in northern California on fracture-induced anisotropy. Nakagome et al. (1998) investigate the Kakkonda geothermal field in Japan and related the weak amplitude zones to increased absorption in fracture zones.

Feighner et al. (1998) identify a coherent reflector that corresponds to a permeable zone responsible for the fluid transport in the Rye Patch geothermal field in Nevada. A VSP and a moving source VSP (MS-VSP) was conducted at Unterhaching in the Munich area to complement surface seismic data (Thomas and Schulz, 2007). It was shown that the VSP had a higher S/N ratio than the surface seismic data and several reflectors could be mapped and fault systems interpreted.

Place et al. (2010, 2011) and Sausse et al. (2010) investigate the geothermal site in Soultz-sous-Forêts in the Upper Rhine Graben with VSP data that was acquired in 1988 and 1993. Diffraction analysis was useful to identify a fault edge and improve the structural interpretation. P-to-S converted wave analysis indicated steeply dipping fracture zones away from the well that control the fluid flow within the granitic basement. An example of the final migrated VSP data is shown in Figure 3.

Review of specialized seismic processing techniques and their potential for geothermal exploration

Over the past few decades, numerous advanced seismic processing techniques have been developed by the oil and gas industry. It remains to be established through detailed testing which of these techniques can be best adapted and profitably applied to geothermal seismic exploration.

Seismic attribute analysis

Seismic attributes are quantities that can be derived from seismic data to extract structural and lithologic information of the subsurface (Chopra and Marfurt, 2005, 2007). There are different ways of classifying a seismic attribute. Taner et al. (1994) divide attributes into geometric and physical attributes. Geometric attributes are normally used in stratigraphic interpretation and enhance geometric characteristics, such as continuity, unconformities, faults, dip, azimuth, and curvature. Physical attributes have a direct link to physical parameters in the subsurface and are generally used for characterization of lithology and reservoirs. Brown (1996) divides attributes into time, amplitude, frequency, and attenuation attributes, which can be further subdivided into pre- and poststack attributes. Prestack amplitudes contain azimuthal and offset information and can be used to determine fluid content and fracture orientation, whereas poststack seismic amplitudes are analyzed on CDP stacked sections and are more suitable for large amounts of data (Taner, 2001).

A classic set of attributes is derived from the complex trace analysis (e.g., reflection strength/instantaneous amplitude, instantaneous frequency; Taner et al., 1979; Chopra and Marfurt, 2005). Reflection strength is sensitive to changes in acoustic impedance and can therefore be used to identify different lithology, porosity, hydrocarbons, and thin-bed tuning. High reflection strength is often related to gas accumulation and may be identified through bright spots. Abrupt changes in reflection strength can also indicate faulting. The instantaneous frequency attribute is a useful tool for lithology characterization, identifying increased attenuation, thin-bed tuning, and as a fracture zone indicator.

Three-dimensional seismic exploration in the 1990s had a profound impact on seismic attribute analysis. A large number of new attributes were developed, and the extraction of stratigraphic information was expanded to exploitation and reservoir characterization (Chopra and Marfurt, 2005). Dip and azimuth maps became two of the most important attributes for identifi-

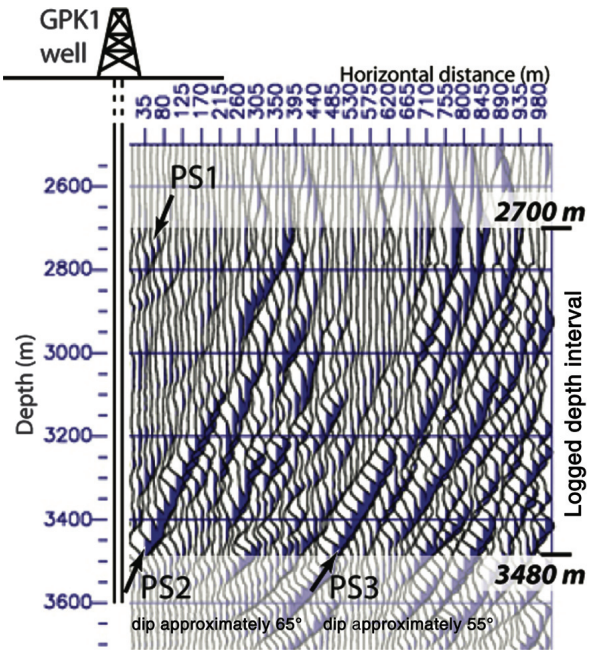

Figure 3. Migrated image of VSP data from Soultz-sous-Fôrets. Steeply dipping reflectors were mapped using P-S converted reflections. Note that the processing did not allow the positioning of reflectors in 3D. Hence, the image is axially symmetric around borehole GPK1. Figure reproduced from Place et al. (2011) (Figure 6). By permission of Oxford University Press on behalf of The Royal Astronomical Society).

cation of faults and other subtle stratigraphic features. Dip and azimuth are the basis for many geometric attributes, e.g., coherence and curvature. Coherence measures the similarity between waveforms and traces and should be computed along local dip and azimuth of a reflector. Coherent regions indicate a laterally continuous lithology, whereas a low degree of coherency indicates discontinuous events, such as faults and fractures. Figure 4 illustrates the utility of coherency maps to locate fracture zones.

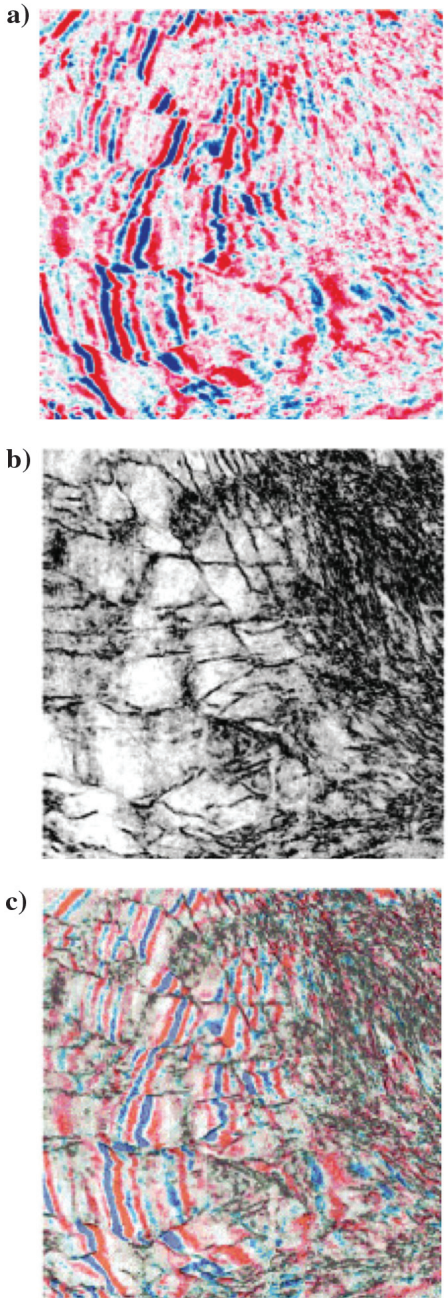

Figure 4. Illustration of the 3D coherence attribute. Time (horizontal) slices through (a) a 3D seismic data cube and (b) coherence data volume. (c) Overlay of panels (a and b). Note how coherence highlights faults and enhances the interpretation of the intensively fractured region to the right (modified after Chopra and Marfurt, 2005).

Applications of attribute analysis in geothermal exploration to enhance the visibility of fracture zones are reported by, for example, von Hartmann et al. (2012) to characterize Upper Jurassic carbonate platforms in southern Germany that could serve as a geothermal reservoir. Different carbonate facies were identified with the help of seismic attribute analysis, such as spectral decomposition. Pussak et al. (2014) extract and analyze root-mean-square (rms) amplitudes, instantaneous frequencies, coherency, and spectral decomposition attributes from a 3D seismic data set to characterize a geothermal reservoir in the Polish Basin with the aim to locate fluid-bearing fracture zones. Seismic attribute analysis is used by Abul Khair et al. (2015) to elucidate deep hot granitic rocks below a thick sedimentary cover at a study site in the Cooper Basin (South Central Australia). The main focus was set on the curvature attribute that enabled the successful imaging of approximately 170 faults that intersect the basement.

Multicomponent (vector) seismic data analysis

The standard practice in land seismic acquisition is to measure the vertical component of the ground motion only. These scalar or 1C data are then processed into P-wave reflectivity or velocity images based on the assumption that the measured 1C records represent mainly P-wave energy (steeply arriving waves polarized in that direction). Multicomponent or vector seismic recordings (measurement with vertical- and horizontal-component geophones; 3C geophones) capture the seismic wavefield more completely than 1C techniques and allow, for example, studying S-waves and mode-converted waves (P-S and S-P conversions; Stewart et al., 2002). The benefits of S-wave and converted-wave exploration are numerous and include "seeing" through gas-bearing sediments, improved fault definition, enhanced near-surface resolution, improved lithologic characterization, subsurface fluid description, and reservoir monitoring (Tatham and McCormack, 1991; Stewart et al., 2003).

Key advantages of multicomponent exploration over 1C data acquisition are the possibility to identify (and separate) the various wave modes based on their polarization properties and to characterize anisotropy by studying S-wave splitting (discussed in detail in the "S-wave birefringence" subsection; Crampin, 1981). Polarization information can be used to determine the direction of different arriving wave types (Vidale, 1986; Rutty and Greenhalgh, 1993) and to provide the possibility for application of polarization filters to, for example, suppress noise or unwanted modes, such as Rayleigh waves (Özbek, 2000), wavefield separation techniques (Dankbaar, 1985; Greenhalgh et al., 1990), and prestack elastic migration (Chang and McMechan, 1994; Zhe and Greenhalgh, 1997). An important motivation of anisotropy studies is the characterization of fracture density and orientation (Crampin, 1985). Fracture characterization is, for example, critical for shale gas

production, which is gaining increasing attention in Europe and worldwide (Weijermars et al., 2011).

Even though land multicomponent seismic exploration gained increased attention during recent years (see, e.g., special sections of *The Leading Edge* in September 2001, December 2003, and January 2013), it remains a niche play, with, for example, P-S-converted wave analysis still only accounting for approximately 5% of the total seismic processing revenue in the exploration seismic industry (Bansal and Gaiser, 2013). In contrast, multicomponent techniques are well established for vertical-seismic profiling. The reasons why multicomponent seismology has not become a widely adopted approach to exploration are the challenging field logistics (e.g., increased number of channels compared with 1C surveys), the requirement of different processing of converted waves compared with P-waves, and difficulties in interpreting the resultant S-wave images (Stewart et al., 2003).

Today, converted-wave acquisition and processing (where sources that generate P-waves are used but where the S-wave converted reflections of these waves at the target are recorded on the surface) is in general deemed to be more practical for oil-and-gas exploration because S-wave sources are large, expensive, and usually have a considerable environmental impact.

Because in high-enthalpy geothermal systems hot steam can be extracted to generate electricity, it is important to locate steam-bearing fracture zones. Steam introduces higher absorption of the seismic wavefield and also has the effect of decreasing the seismic velocity. Wei et al. (2014a, 2014b) show the benefits of using multicomponent seismic data in the Wister geothermal field, which is a Cenozoic sedimentary basin located in California. The goal of their study was to evaluate potential reservoir units, locate fault, and fracture zones and investigate whether additional value can be gained from multicomponent seismic data. It was shown that V_P/V_S velocity ratios were beneficial to identify and specify different rock types, and that P-SV data were more sensitive to fractures than P-P data, particularly in hot steam-filled sections. Because P-waves get strongly attenuated by gas-filled pores, P-SV images can significantly improve the image quality within and below the gas-filled formation (Figure 5).

S-wave birefringence

When S-waves encounter an anisotropic medium they show very different characteristics in comparison with P-waves (Tsvankin, 2012). The S-wave splits into fast and slow S-wave components having orthogonal polarizations, which are normal to the wave direction (the same as that of the incident S-wave), whereas the P-wave is less affected by the anisotropy and does not separate (Crampin, 1981, 1985; Hardage et al., 2011). The S-wave splitting can be caused by different anisotropic conditions, such as aligned crystals, stress-induced anisotropy, lithologic anisotropy, structural anisotropy, and crack-induced anisotropy (Crampin and Lovell, 1991). In a fractured medium, the polarization of the fast S-wave is oriented parallel to the fracture plane and the slow S-wave shows particle motion perpendicular to the fracture plane. The idea that S-wave splitting can be used for fracture characterization lead to several successful studies in hydrocarbon exploration. It was shown that S-wave birefringence can be used for fracture mapping and that higher anisotropy can be correlated with increased oil production rates (Cliet et al., 1991).

Because S-waves split whenever they are propagating through an anisotropic medium, the observed polarization can also be induced through the anisotropy

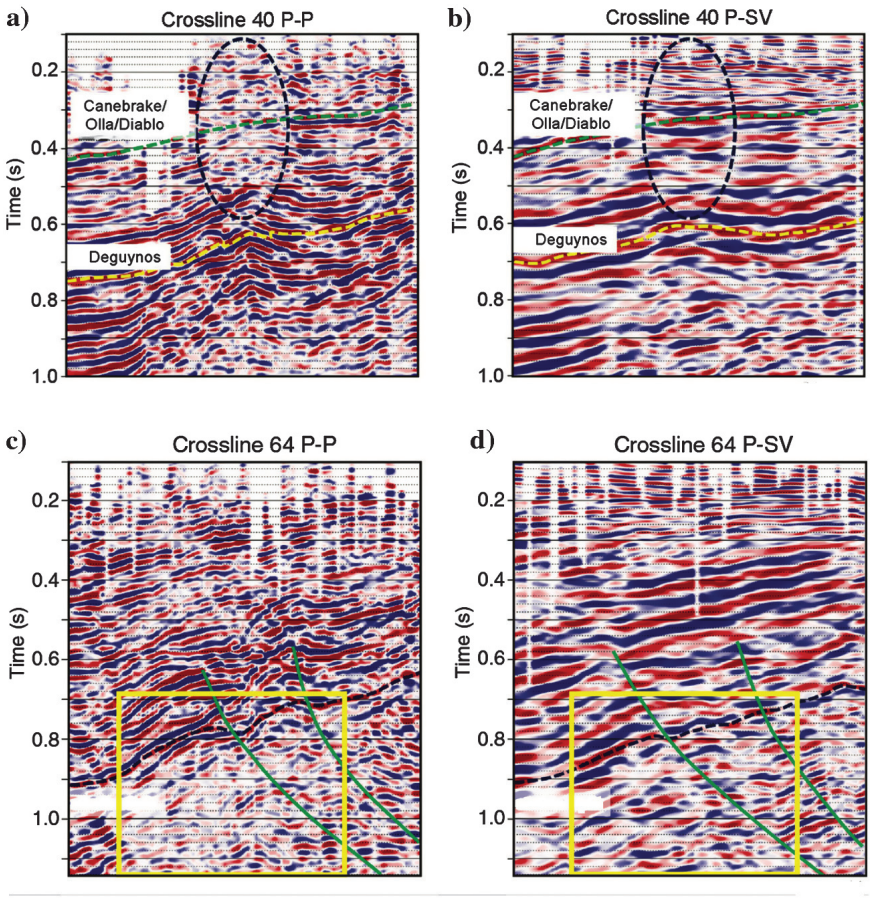

Figure 5. Seismic section that illustrates (a and b) differences between P-P and P-SV stacks within gas clouds marked by black ovals and (c and d) across a region with low saturation of high-temperature fluid indicated with a yellow rectangle. Note that P-SV data contain more amplitude information within gas clouds and fluid-filled regions compared with P-P data (modified from Wei et al., 2014a).

of the overburden layer. Yardley and Crampin (1991) suggest the use of VSP surveys to analyze S-wave splitting to avoid the problem of the near-surface layer. It was shown that VSPs are less affected by the surface overburden and that the recorded polarization was dominated by the anisotropy of the rock in the vicinity of the borehole.

The time difference between the fast and slow S-waves is affected by the propagation distance and direction as well as the degree of anisotropy (Li and Mueller, 1997). Because fracture density is mainly responsible for the degree of anisotropy, the time delay can be used to estimate fracture density (Lewis et al., 1991). The time delay is normally determined by comparing slow and fast S-wave stacked sections. In a study by Hitchings and Potters (2000), a fractured carbonate reservoir is examined by analyzing time delays between fast and slow S-waves. Regions with larger time delays indicate increased anisotropy, which corresponded to higher fracture density (Figure 6).

S-wave splitting in geothermal fields has so far been analyzed by using natural and induced seismic events. Because the time delay between the fast and slow S-wave is proportional to the crack density, S-wave birefringence is a valuable tool to characterize fractures in geothermal fields. Case studies in the Coso geothermal field in the Sierra Nevada Range, The Geysers geothermal site near the San Andreas Fault, and the Krafla site in northern Iceland show that polarization and time delay analyses of microearthquakes can be used to detect orientation and fracture density (Rial et al., 2005; Tang et al., 2008).

Estimating fracture orientation and fracture density as well as understanding the stress state of the subsurface is of great importance in geothermal exploration. The information could be used not only to identify regions with larger hydraulic conductivity, but also to predict directions of hydraulic fracturing. This would provide further constraints on the location and design of geothermal wells. Analyzing fast and slow S-waves on VSP data could therefore provide additional information on fracture orientation and intensity in the subsurface.

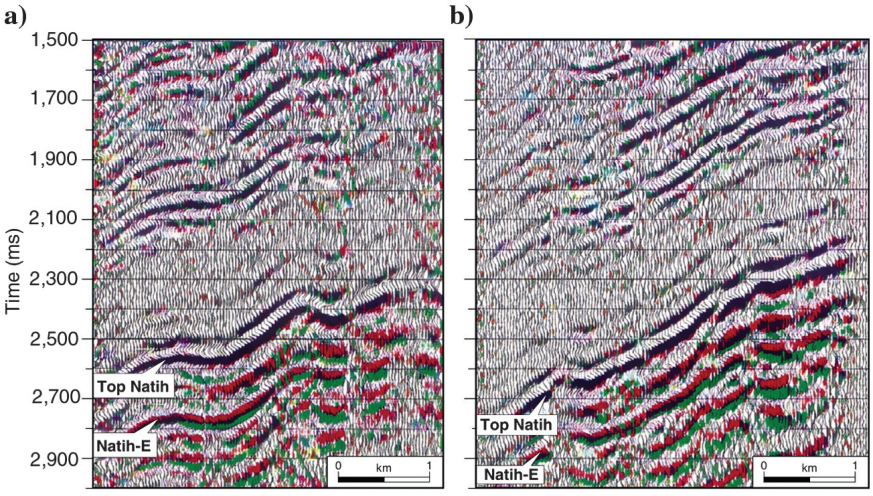

Figure 6. Processed split S-wave profiles (a and b) over a fractured carbonate reservoir (top and bottom is labeled), after Hitchings and Potters (2000). Red corresponds to the fast S-wave response, green corresponds to the slow S-wave response, and black corresponds to the common response. Time delays within the reservoir increases from left to right, indicating increased fracture density.

Diffraction imaging

For the basement targets of importance in geothermal exploration (e.g., fracture planes, shear zones, fluid pathways, faults) the velocity contrasts are likely to be small, the dips steep, and the surface areas of the reflectors small. This leads to signal amplitudes that are typically one-fifth or less that of reflections from laterally continuous layers encountered in the sedimentary section above. The detection and identification of such small diffraction signatures places severe demands on seismic field and processing practice. For example, detectability is frequency (wavelength) dependent. The lower the dominant frequency, the harder it is to detect a target feature. The higher the dominant frequency, the greater the wave absorption and the more difficult the field procedures and data processing become.

The ratio of the surface area of the body to the first Fresnel zone determines the horizontal detectable limit. A reflector is considered to be detectable if the ratio exceeds 0.05. For the most part it is expected that the geothermal targets will have a complex shape and spatial dimensions that are comparable with (or smaller than) the Fresnel zone associated with the source frequencies (typically <50 Hz, but sometimes as high as 90 Hz) used and the target depth (3–5 km). Thus, they fall within the so-called Mie scattering regime, and common tools of the trade such as ray tracing are inappropriate for predicting their seismic expression. Full-wave theoretic modeling is required (e.g., finite-difference modeling; Robertsson and Blanch, 2011). The shape of the reflector itself will exert a first-order control on the P-wave scattering response. Unlike point diffractors, dipping lenticular or ellipsoidal fractures are expected to focus scattered P-waves in the long axis (specular reflection) direction, down dip from the feature (Bohlen et al., 2003).

It is generally appreciated that with the surface-based CDP (P-wave) reflection technique, steeply dipping, and irregular interfaces are difficult to detect and image. The folded and faulted nature of the host rock in basement terrains means that there is a lack of bed continuity and marker horizons. One obvious approach is to concentrate on the diffracted portion of the wavefield, which can offer superior or even super-resolution compared with reflection imaging (Moser and Howard, 2008). The high-resolution (subwavelength) infor-

mation encoded in diffractions is generally lost during conventional processing. In contrast, diffraction imaging makes it possible to map small-scale discontinuous subsurface objects. Processing techniques to decompose the specular and diffraction (diffuse) energy from the total scattered wavefield have been presented by several researchers in recent years (Landa and Keydar, 1998; Khaidukov et al., 2004; Klokov and Fomel, 2012). They are generally based on the ability to decompose the recorded wavefield into continuous full azimuth and dip directivity components in situ at the subsurface points. The technique takes advantage of the kinematic differences of the scattered and reflected seismic energy. Other techniques such as those proposed by Schmelzbach et al. (2008a) and Malehmir et al. (2009) use a scheme that measures similarity along diffraction traveltime curves to map the location of point diffractors due to faults/fractures and suspected ore bodies, respectively, in crystalline rocks. This is illustrated in Figure 7.

Velocity model building

It is standard practice in reflection seismic processing to undertake a semblance-type velocity analysis to identify multiples, estimate interval velocities, and perform a time/depth conversion. Migration velocity analysis to obtain the macro-velocity field is also required for effective imaging, such as post- and prestack migration. The derived interval velocities can also be used for geologic and petrological interpretations, such as discerning rock type, rock condition, and fluid content (Lüschen et al., 2014, 2015). In the following two sections, we describe two other sophisticated methods for velocity model building — traveltime tomography and full-waveform inversion (FWI).

Traveltime tomography

The aim of seismic ray tomography is to find a subsurface velocity model that can explain the first-arrival traveltimes. During the inversion process, the calculated traveltimes are compared with the actual traveltimes, and the velocity model is iteratively modified until the traveltime differences lie within the measurement error (Lanz et al., 1998; Zelt and Barton, 1998; Rawlinson and Sambridge, 2003).

Classical ray tomography is based on the high-frequency assumption, which means that the ray is taken to be infinitely thin and not affected by diffraction and scattering from the surrounding rock. Wave-equation tomography was introduced by Pratt and Goulty (1991) and Woodward (1992). Wave-equation tomography is a subset of FWI and does not rely on the high-frequency assumption and should therefore provide higher resolution images. However, the source wavelet needs to be adequately known for the wavefield calculation and it further assumes the recorded data to be noise free.

Fat ray tomography represents a compromise between classical ray tomography and wave-equation tomography (Vasco et al., 1995; Husen and Kissling, 2001; Jordi et al., 2016). The ray is not assumed to be

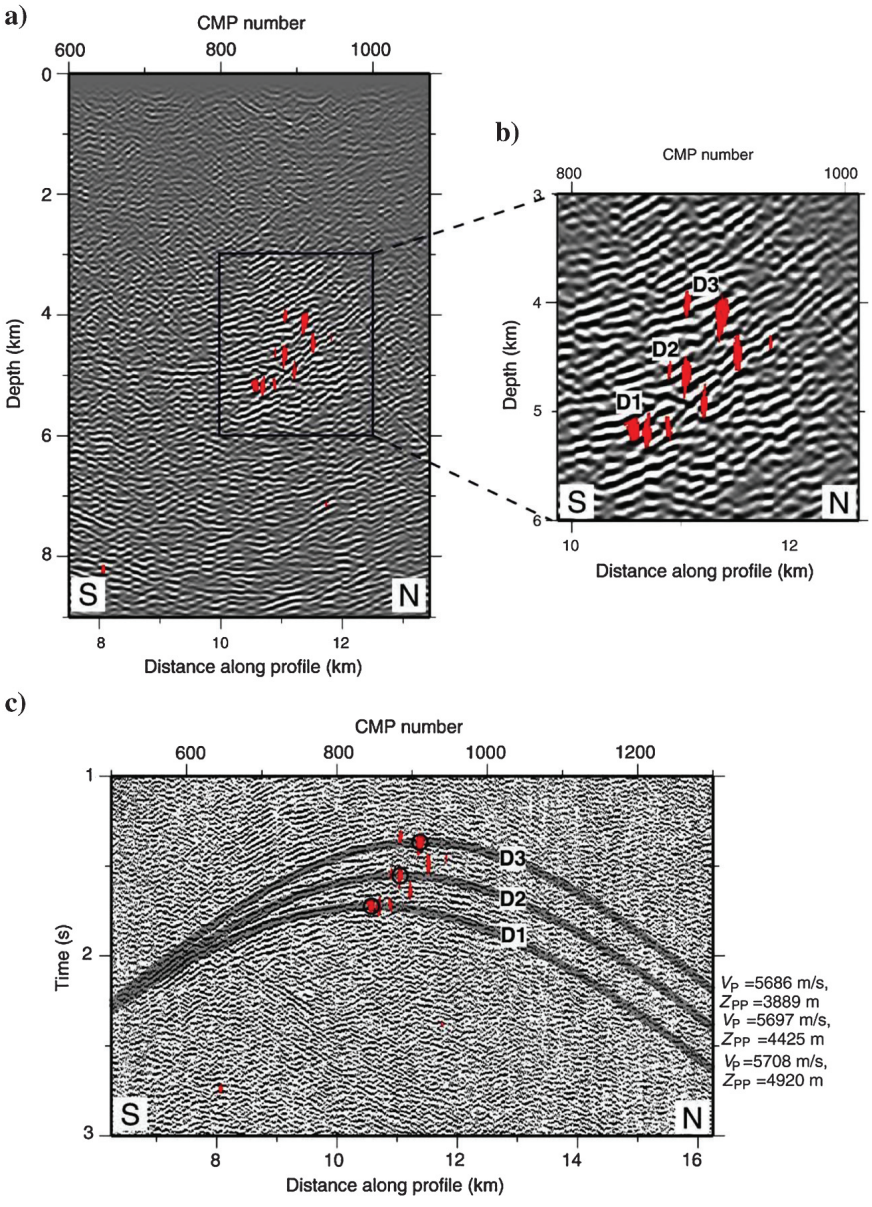

Figure 7. Diffraction imaging in crystalline rocks. (a) Diffracting elements plotted in red onto migrated and depth-converted 2D seismic section. (b) Close-up view of panel (a). (c) Simulated traveltime curves (gray) for three diffractors shown in red are plotted onto the unmigrated data. Note that the synthetic traveltime curves match reasonably well with the observed diffraction patterns. Figure reprinted from Malehmir et al. (2009), copyright (2009), with permission from Elsevier.

infinitely thin, but takes the frequency-dependent size of the first Fresnel zone into account for the wave propagation. Scattering within the Fresnel volume results in constructive interference of the seismic signal. Due to a more realistic description of seismic wave propagation, enhanced subsurface imaging is expected. Fat ray tomography is expected to increase the imaging capability in terms of additional subsurface information, improved resolution, and better localization of low-velocity zones due to the more realistic description of the seismic wave propagation. Fat ray tomography can be very beneficial in that it can provide an advanced macro-velocity model for migration, statics analysis, and a suitable starting model for FWI.

Crosshole (borehole-to-borehole) traveltime seismic tomography is often applied to image the velocity structure between wells, with applications including orebody delineation (Greenhalgh et al., 2003) and hydrocarbon-reservoir monitoring (Spetzler et al., 2008). If the rocks are anisotropic, the tomography formulation has to be adapted, otherwise the isotropic velocity tomograms can be severely distorted (Pratt et al., 1993). Several approaches have been proposed to handle anisotropy in crosshole seismic tomography, differing in simplifying assumptions and parameterization of anisotropy (Chapman and Pratt, 1992; Zhou et al., 2008). Vécsey et al. (1998) demonstrate that accounting for anisotropy in crosshole measurements at a potential hot dry rock reservoir to monitor effects of changing fluid pressure greatly enhanced the interpretability of the tomograms.

Full-waveform inversion

FWI is an imaging method that seeks to exploit simultaneously the whole seismic data along each trace to reconstruct high-resolution quantitative images of the characteristic parameters (seismic velocities, density, and attenuation) of large areas of the subsurface. Because the entire seismograms are used for FWI, the most complete representation of the subsurface is expected. Thus, FWI is expected to provide quantitative images with the resolution of migration and diffraction imaging (half of the shortest wavelength expected for favorable illumination). Comprehensive reviews of the method are given by, for example, Virieux and Operto (2009) and Fichtner (2011).

However, the development of FWI has faced several major challenges:

1) The accurate numerical forward modeling of the full 3D viscoelastic wave propagation in a very complex and arbitrary medium including composite features, such as faults, free surface with topography, attenuation and anisotropy is a difficult task, and requires extremely intensive computational facilities.
2) The associated inverse problem is highly nonlinear, in particular for the high frequencies and in the seismic reflection configuration. Indeed, the prior knowledge of the large-scale variations of the medium is necessary. This information is given through a reference background (initial) velocity model that can be obtained, for instance, by velocity analysis, or refraction or reflection traveltime tomography.

Due to these difficulties, FWI has been applied in a restricted, sequential, and simplified manner over the past 30 years. Several approaches have been proposed to mitigate the nonlinearity of the inverse problem starting, for example, by inverting first the low-frequency information of the data before progressing to higher frequencies (Sirgue and Pratt, 2004; Brossier et al., 2009).

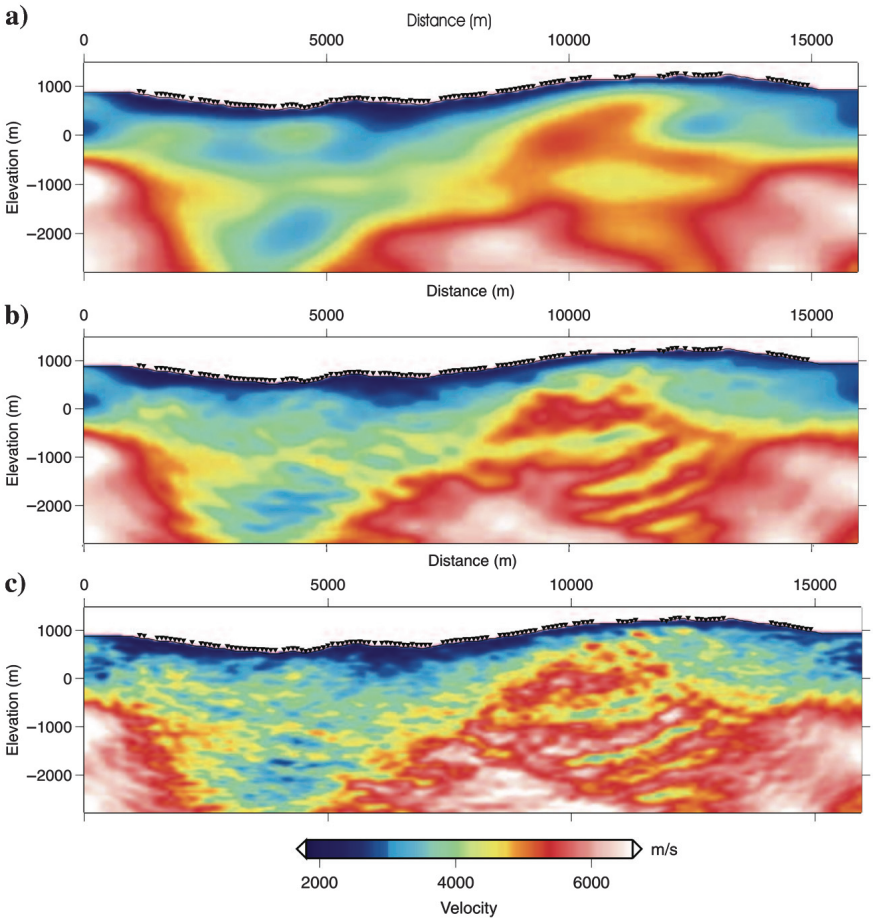

Figure 8. (a) Velocity model from traveltime tomography. This model was used as a starting model for the full-waveform tomography. (b) Velocity model from full-waveform tomography after the inversion of the 5.4 and (c) 20.06 Hz components. Note the improvement in spatial resolution from panels (a-c). The triangles in panels (a-c) mark the receiver positions involved in the tomography (modified after Operto et al., 2004).

Initially, FWI was proposed for 2D acoustic data in the time domain (Tarantola, 1984; Crase et al., 1990) and later developed for reasons of computational efficiency in the frequency domain (Pratt, 1999; Pratt and Shipp, 1999). Wide-angle refraction data have been used in several studies to build initial models using first-arrival traveltime tomography and then to invert the data using acoustic FWI (Dessa, 2004; Operto et al., 2004; Malinowski et al., 2011). One approach of inverting wide-angle refraction data is early arrivals waveform inversion (EAWI), which provides higher resolution than traveltime tomography but is still restricted to the use of refracted and early arrival reflected and diffracted waves, and thus limited in investigation depth. Figure 8 shows an example of EAWI illustrating the improved resolution compared with traveltime tomography.

The problem of constructing an accurate initial model is less pronounced in the transmission configuration (crosshole and VSP experiments) because the inverse problem is more linear when using transmitted (forward scattered) waves compared with reflected (back-scattered) waves. Furthermore, traveltime tomography can be used in crosshole surveys to obtain a consistent and accurate initial model, and possibly borehole logs can be used to constrain the inversion. Several studies illustrate the value of FWI for crosshole acquisition geometries (Pratt and Goulty, 1991; Manukyan et al., 2012).

With the evolution and improvement of computing facilities in recent years, 3D inversion has become feasible under the acoustic approximation and has been successfully applied on marine data sets (Sirgue et al., 2009; Figure 9). Today, 3D time-domain viscoelastic inversion has become feasible in exploration seismics (Vigh et al., 2014; Raknes et al., 2015), and it is also being progressively applied at the regional and global scale using earthquake sources (Fichtner et al., 2008, 2010). In general, the lithospheric and regional imaging using FWI is easier to solve than FWI of exploration-scale data because accurate background velocity, density, and attenuation models are usually known, and the problem is more linear because the velocity contrasts are smaller and mainly transmitted surface waves are inverted.

Current developments on the exploration-scale seek to combine FWI and wave-equation migration velocity analysis (Symes, 2008). Constant improvements are being made in modeling accuracy and efficiency, for models incorporating anisotropy, attenuation, and high impedance contrasts. Solutions have also been developed to better address the reconstruction of multiple

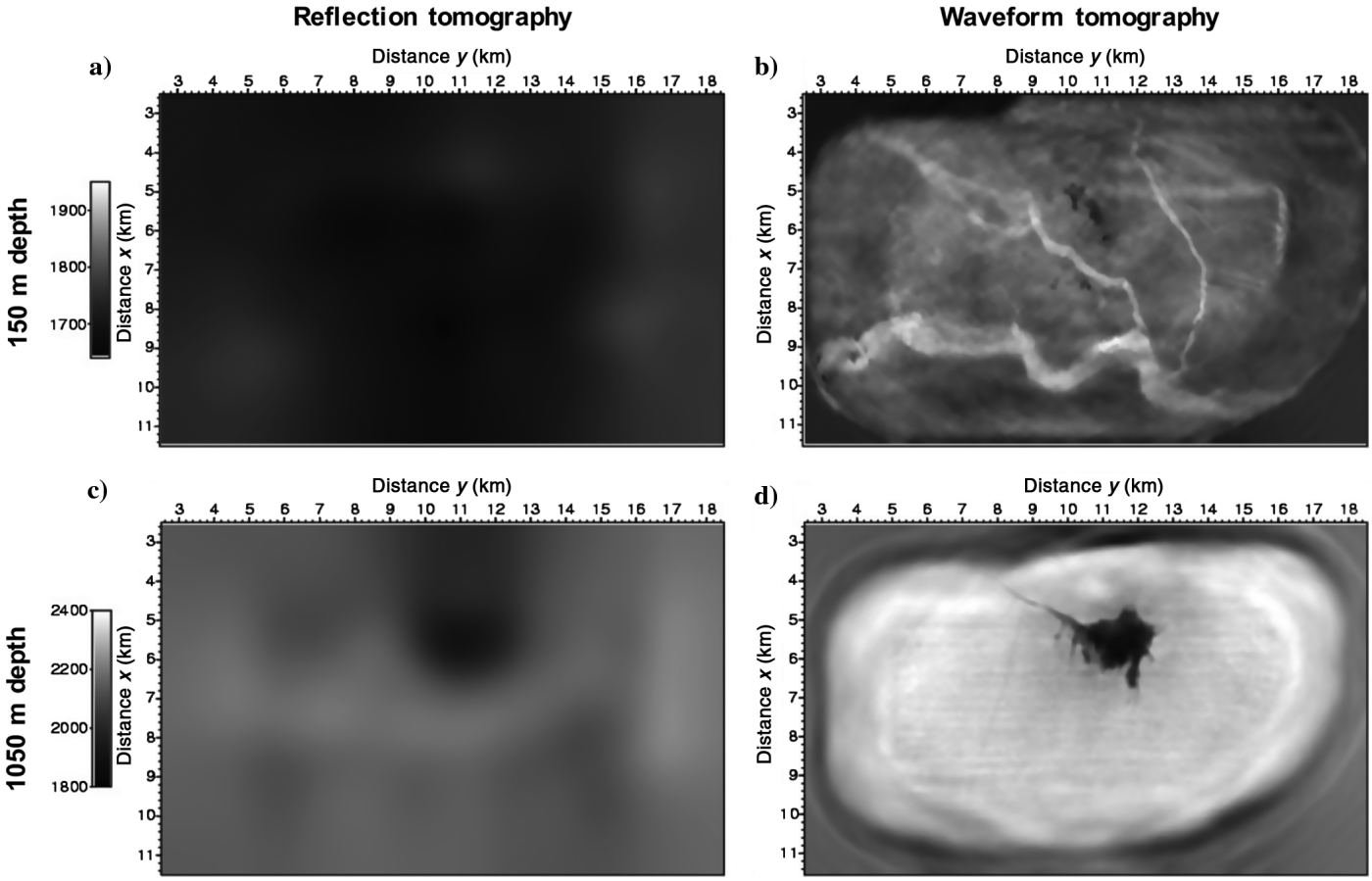

Figure 9. Example of 3D waveform inversion applied to wide-azimuth ocean-bottom cable data from the Valhall field. Horizontal slices through a 3D velocity model at (a and b) 150 m depth, and (c and d) 1050 m depth for (a and c) the reflection tomography and (b and d) the waveform inversion results (after Sirgue et al., 2009).

parameters during the inversion (Malinowski et al., 2011; Manukyan et al., 2012; Alkhalifah and Plessix, 2014; Vigh et al., 2014).

To date, FWI has not been used for geothermal exploration. As the exploration depth and surface illumination configurations are similar to oil and gas exploration, application of FWI to geothermal targets can benefit from all the developments made for oil prospecting, but will still be subject to the same difficulties and limitations (cost of forward modeling, construction of an accurate initial model for velocity, density, and attenuation, data preprocessing or transformation when the modeling relies on strong assumptions such as acoustic propagation only). The benefit of using FWI for geothermal exploration is at least an improvement of the structural imaging, for example, when FWI-derived velocity information is used for prestack migration. The application of FWI for quantitative imaging is more challenging, and will clearly depend on the ability to build reliable initial velocity and density models. Elastic FWI may provide high-resolution spatial distributions of elastic parameters, which can be linked to intrinsic physical properties, such as porosity and saturation. If the velocity model is well constrained, then it is also possible to expect quantitative estimation of attenuation variations, as shown, for instance, by Hicks and Pratt (2001) and Malinowski et al. (2011). Simultaneous P- and S-wave attenuation imaging potentially provides information on temperature variations and fluid saturation. Temperature increases are known from laboratory investigations and crustal/upper mantle seismic field studies to lower the seismic wave speed and increase the attenuation (Schön, 1996). However, it is often extremely difficult to nigh impossible to isolate small seismic anomalies due to moderate temperature changes from other factors, such as stress, compositional changes, and fluid effects.

Another potential use of FWI in the context of geothermal exploration and production is time-lapse (4D) monitoring of small changes in the subsurface. Once a baseline velocity model has been constructed, the differences between the full seismic data at two or more different times can be inverted to obtain a quantitative estimation of the changes in the model (Raknes and Arntsen, 2015).

Conclusions

Seismic reflection imaging has a greater depth of penetration combined with reasonable resolution compared with other geophysical methods used to study geothermal reservoirs. Yet, seismic imaging has only sparingly been used for geothermal exploration and it needs to be investigated how established and recently developed seismic data analysis techniques can be adapted and successfully applied to geothermal sites.

EGS will mostly be located in hard rock (basement) rather than the sedimentary rocks. Because the impedance contrasts and reflection coefficients between most crystalline lithologies are smaller than those of sedimentary lithologies, the S/N will be low, making it more difficult to image structures (e.g., fracture zones) in the basement. Moreover, the target reflectors are likely to be rough and of limited spatial extent, further reducing signal amplitudes and exacerbating their detection and delineation. Consequently, particular care must be taken in survey planning, acquisition, and processing to maximize the S/N.

The structures of importance in geothermal exploration in hard-rock environments are expected to be complex in shape and steeply dipping, which means that the reflections will tend to arrive at the surface in unexpected locations. In some cases, borehole measurements (e.g., multicomponent VSPs) may be better suited to image steeply dipping features than surface-based surveys. It will be necessary to model surveys beforehand in future seismic experiments to determine optimum locations for sources and receivers, to improve the processing, and to aid with the interpretation of the data. The targets (e.g., fracture zones) are small and will more likely appear as diffractions rather than as reflections on seismic profiles.

Most existing reflection seismic data over potential geothermal fields data were acquired for hydrocarbon exploration purposes, where the survey layout was designed to image the sedimentary column above the crystalline basement. The recording apertures (maximum source-receiver distances) and azimuths are mostly inadequate for imaging steep dips within the basement. Very few successful geothermal-specific seismic reflection surveys have been carried out in the past. Future surveys will require every degree of sophistication that can be brought to bear. The vast experience of oilfield seismic imaging has much to offer in illuminating the route toward improved seismic exploration of geothermal reservoirs — but the geothermal problem is special and comes with its own set of particular considerations. The major technical modifications need to be in the use of 3D arrays and multicomponent sensors, coupled with sophisticated processing, including attribute analysis, polarization filtering/migration, and the separation of diffracted and specular reflected wavefields. For example, attributes like azimuth and dip attributes, coherency, curvature, and spectral decomposition as well as other attributes could be further tested to evaluate the potential for fracture mapping not only in deep sediments but also in crystalline basement. FWI and S-wave splitting investigations can be profitably carried out provided that the data are of sufficient quality and potentially provide quantitative estimates of elastic parameters, from which it may be possible to infer critical reservoir properties, such as porosity and temperature.

The road ahead via complementary measurements

There are several remaining challenges and areas of active seismic reflection imaging research that may potentially become important to geothermal exploration in the future. A few of them are discussed here. A major

challenge in land-seismic acquisition is the impact of the earth's near-surface zone (upper 10s–100s of m) on seismic data recorded on land due to its complexity and heterogeneity. This near-surface impact includes distortions of signals caused by irregular time delays, scattering, and absorption in the near-surface layer(s) and consequent loss of high-frequency information, the generation of coherent surface-related noise (e.g., ground roll, guided waves; Robertsson et al., 1996), and signal amplitude and phase changes due to rapid lateral near-surface variations. Although many approaches have been developed to, for example, correct for static (time) delays and to remove source-generated noise (Yilmaz, 2001), being able to satisfactorily remove or correct for the distortions caused by the near-surface zone remains a major challenge.

A central goal in geophysical exploration is to build accurate subsurface models that include quantitative estimates of rock properties and fluid content at different scales. Combining complementary geophysical data sets by joint or cooperative inversion and/or interpretation, for example, acquired with different geophysical methods typically reduces ambiguities and facilitates the interpretation. Joint inversion has been used to improve the classification of lithologic zones and to establish petrophysical relationships on different scales (Colombo and De Stefano, 2007; Colombo et al., 2014). Muñoz et al. (2010) use statistical joint interpretation of electrical resistivity and seismic velocity model to characterize different units at the Groß Schönebeck (Germany) geothermal site in terms of lithology and fracturing.

Microseismic data analysis and interpretation are receiving increasing attention for subsurface exploration and monitoring of hydrocarbon and geothermal reservoirs. If microseismic waveforms are recorded with dense enough receiver layouts, then these data may be analyzed with state-of-the-art seismic imaging and inversion techniques. Reflections identified within the coda of microseismic recordings may be used for imaging of subsurface structures (Schmelzbach et al., 2016). Considering the usually broad frequency content and the short travel paths between microseismic events and borehole and/or surface-based receivers, the seismic-reflection processing of microseismic waveform recordings is a promising approach for high-resolution subsurface characterization. Reshetnikov et al. (2015) process microseismic waveforms recorded during and after the stimulation of the EGS in Basel, Switzerland, to map a distinct network of reflectors in the vicinity of the injection well.

Acknowledgments

We thank the CARNEVAL consortium sponsors Nagra, OMV, and Schlumberger Gould Research for partial support of C. Schmelzbach. We appreciate constructive comments by J. Reinecker, E. Lüschen, M. Jud, and S. Buske that helped in improving the quality of this paper. We thank all the copyright holders for granting permission to reproduce figures (Laurent Sirgue, Oxford University Press, Elsevier, Wiley, SEG, and EAGE). The research leading to these results has received funding from the European Community's Seventh Framework Programme under grant agreement 608553 (Project IMAGE).

References

Abul Khair, H., D. Cooke, and M. Hand, 2015, Seismic mapping and geomechanical analyses of faults within deep hot granites, a workflow for enhanced geothermal system projects: Geothermics, **53**, 46–56, doi: 10.1016/j.geothermics.2014.04.007.

Adam, E., T. Bohlen, and B. Milkereit, 2003, Vertical seismic profiling at the Bell Allard Orebody, Matagami, Québec, *in* D. W. Eaton, B. Milkereit, and M. H. Salisbury, eds., Hardrock seismic exploration: SEG, 181–193.

Ahmed, K. A., B. Schwarz, and D. Gajewski, 2015, Application of the 3D common-reflection-surface stack workflow in a crystalline rock environment: 3D CRS in crystalline environment: Geophysical Prospecting, **63**, 990–998, doi: 10.1111/1365-2478.12282.

Alkhalifah, T., and R.-É. Plessix, 2014, A recipe for practical full-waveform inversion in anisotropic media: An analytical parameter resolution study: Geophysics, **79**, no. 3, R91–R101, doi: 10.1190/geo2013-0366.1.

Arnórsson, S., 1995, Geothermal systems in Iceland: Structure and conceptual models — I. High-temperature areas: Geothermics, **24**, 561–602, doi: 10.1016/0375-6505(95)00025-9.

Bansal, R., and J. Gaiser, 2013, An introduction to this special section: Applications and challenges in shear-wave exploration: The Leading Edge, **32**, 12, doi: 10.1190/tle32010012.1.

Barbier, E., 2002, Geothermal energy technology and current status: An overview: Renewable and Sustainable Energy Reviews, **6**, 3–65, doi: 10.1016/S1364-0321(02)00002-3.

Bellefleur, G., C. Müller, D. Snyder, and L. Matthews, 2004, Downhole seismic imaging of a massive sulfide orebody with mode-converted waves, Halfmile lake, New Brunswick, Canada: Geophysics, **69**, 318–329, doi: 10.1190/1.1707051.

Bohlen, T., C. Müller, and B. Milkereit, 2003, 5. Elastic seismic-wave scattering from massive sulfide orebodies: On the role of composition and shape, *in* D. W. Eaton, B. Milkereit, and M. H. Salisbury, eds., Hardrock seismic exploration: SEG, 70–89.

Brogi, A., A. Lazzarotto, D. Liotta, and G. Ranalli, 2005, Crustal structures in the geothermal areas of southern Tuscany (Italy): Insights from the CROP 18 deep seismic reflection lines: Journal of Volcanology and Geothermal Research, **148**, 60–80, doi: 10.1016/j.jvolgeores.2005.03.014.

Brossier, R., S. Operto, and J. Virieux, 2009, Seismic imaging of complex onshore structures by 2D elastic frequency-domain full-waveform inversion: Geophysics, **74**, no. 6, WCC105–WCC118, doi: 10.1190/1.3215771.

Brown, A. R., 1996, Seismic attributes and their classification: The Leading Edge, **15**, 1090–1090, doi: 10.1190/1.1437208.

Brown, A. R., 2004, Interpretation of three-dimensional seismic data: AAPG Memoir 42.

Buness, H. A., H. von Hartmann, H.-M. Rumpel, C. M. Krawczyk, and R. Schulz, 2014, Fault imaging in sparsely sampled 3D seismic data using common-reflection-surface processing and attribute analysis — A study in the Upper Rhine Graben: Fault imaging in sparsely sampled 3D seismic data: Geophysical Prospecting, **62**, 443–452, doi: 10.1111/1365-2478.12099.

Carr, B. J., S. B. Smithson, N. Kareav, A. Ronin, V. Garipov, Y. Kristofferson, P. Digranes, D. Smythe, and C. Gillen, 1996, Vertical seismic profile results from the Kola Superdeep Borehole, Russia: Tectonophysics, **264**, 295–307, doi: 10.1016/S0040-1951(96)00133-3.

Chang, W., and G. A. McMechan, 1994, 3-D elastic prestack, reverse-time depth migration: Geophysics, **59**, 597–609, doi: 10.1190/1.1443620.

Chapman, C. H., and R. G. Pratt, 1992, Traveltime tomography in anisotropic media — I. Theory: Geophysical Journal International, **109**, 1–19, doi: 10.1111/j.1365-246X.1992.tb00075.x.

Chopra, S., and K. J. Marfurt, 2005, Seismic attributes — A historical perspective: Geophysics, **70**, no. 5, 3SO–28SO, doi: 10.1190/1.2098670.

Chopra, S., and K. J. Marfurt, 2007, Seismic attributes for prospect identification and reservoir characterization: SEG and EAGE.

Chopra, P., and D. Wyborn, 2003, Australia's first hot dry rock geothermal energy extraction project is up and running in granite beneath the Cooper Basin, NE South Australia: Proceedings of the Ishihara Symposium: Granites and Associated Metallogenesis, 43–45.

Cliet, C., A. Tikhonov, D. Marin, and D. Michon, 1991, Anisotropy survey for reservoir definition: Geophysical Journal International, **107**, 417–427, doi: 10.1111/j.1365-246X.1991.tb01403.x.

Clowes, R. M., A. G. Green, C. J. Yorath, E. R. Kanasewich, G. F. West, and G. D. Garland, 1984, LITHOPROBE — A national program for studying the third dimension of geology: Journal of the Canadian Society of Exploration Geophysicists, **20**, 23–39.

Colombo, D., and M. De Stefano, 2007, Geophysical modeling via simultaneous joint inversion of seismic, gravity, and electromagnetic data: Application to prestack depth imaging: The Leading Edge, **26**, 326–331, doi: 10.1190/1.2715057.

Colombo, D., G. McNeice, N. Raterman, M. Zinger, D. Rovetta, and E. Sandoval Curiel, 2014, Exploration beyond seismic: The role of electromagnetics and gravity gradiometry in deep water subsalt plays of the Red Sea: Interpretation, **2**, no. 3, SH33–SH53, doi: 10.1190/INT-2013-0149.1.

Cook, F. A., A. J. van der Velden, K. W. Hall, and B. J. Roberts, 1999, Frozen subduction in Canada's Northwest Territories: Lithoprobe deep lithospheric reflection profiling of the western Canadian Shield: Tectonics, **18**, 1–24.

Cosma, C., P. Heikkinen, and J. Keskinen, 2003, Multiazimuth VSP for rock characterization of deep nuclear waste disposal sites in Finland, *in* D. W. Eaton, B. Milkereit, and M. H. Salisbury, eds., Hardrock seismic exploration: SEG, 207–226.

Crampin, S., 1981, A review of wave motion in anisotropic and cracked elastic-media: Wave Motion, **3**, 343–391, doi: 10.1016/0165-2125(81)90026-3.

Crampin, S., 1985, Evaluation of anisotropy by shear-wave splitting: Geophysics, **50**, 142–152, doi: 10.1190/1.1441824.

Crampin, S., and J. H. Lovell, 1991, A decade of shear-wave splitting in the Earth's crust: What does it mean? what use can we make of it? and what should we do next?: Geophysical Journal International, **107**, 387–407, doi: 10.1111/j.1365-246X.1991.tb01401.x.

Crase, E., A. Pica, M. Noble, J. McDonald, and A. Tarantola, 1990, Robust elastic nonlinear waveform inversion: Application to real data: Geophysics, **55**, 527–538, doi: 10.1190/1.1442864.

Dankbaar, J. W. M., 1985, Separation of P- and S-waves: Geophysical Prospecting, **33**, 970–986, doi: 10.1111/j.1365-2478.1985.tb00792.x.

Dessa, J.-X., 2004, Multiscale seismic imaging of the eastern Nankai trough by full waveform inversion: Geophysical Research Letters, **31**, L18606, doi: 10.1029/2004GL020453.

Drummond, B. J., A. J. Owen, J. C. Jackson, B. R. Goleby, and S. N. Sheard, 2003, Seismic-reflection imaging of the environment around the Mount Isa Orebodies, Northern Australia: A case study, *in* D. W. Eaton, B. Milkereit, and M. H. Salisbury, eds., Hardrock seismic exploration: SEG, 127–138.

Duchane, D., and D. Brown, 2002, Hot dry rock (HDR) geothermal energy research and development at Fenton Hill, New Mexico: Geo-Heat Centre Quarterly Bulletin, **23**, 13–19.

Eaton, D. W., B. Milkereit, and M. H. Salisbury, eds., 2003, Hardrock seismic exploration: SEG, Geophysical Development Series.

Emsley, S. J., P. Shiner, N. Enescu, A. Beccacini, and C. Cosma, 2007, Using VSP surveys to bridge the scale gap between well and seismic data: Geological Society, London, Special Publications, **270**, 83–91, doi: 10.1144/GSL.SP.2007.270.01.06.

Feighner, M. A., T. M. Daley, and E. L. Majer, 1998, Results of vertical seismic profiling at Well 46-28, Rye Patch geothermal field, Pershing County, Nevada, LBNL-41800: Lawrence Berkeley National Laboratory.

Fichtner, A., 2011, Full seismic waveform modelling and inversion: Springer, Advances in geophysical and environmental mechanics and mathematics 343.

Fichtner, A., B. L. N. Kennett, H. Igel, and H.-P. Bunge, 2008, Theoretical background for continental- and global-scale full-waveform inversion in the time-frequency domain:

Geophysical Journal International, **175**, 665–685, doi: 10.1111/j.1365-246X.2008.03923.x.

Fichtner, A., B. L. N. Kennett, H. Igel, and H.-P. Bunge, 2010, Full waveform tomography for radially anisotropic structure: New insights into present and past states of the Australasian upper mantle: Earth and Planetary Science Letters, **290**, 270–280, doi: 10.1016/j.epsl.2009.12.003.

Genter, A., K. Evans, N. Cuenot, D. Fritsch, and B. Sanjuan, 2010, Contribution of the exploration of deep crystalline fractured reservoir of Soultz to the knowledge of enhanced geothermal systems (EGS): Comptes Rendus Geoscience, **342**, 502–516, doi: 10.1016/j.crte.2010.01.006.

Gérard, A., A. Genter, T. Kohl, P. Lutz, P. Rose, and F. Rummel, 2006, The deep EGS (Enhanced Geothermal System) project at Soultz-sous-Forêts (Alsace, France): Geothermics, **35**, 473–483, doi: 10.1016/j.geothermics.2006.12.001.

Greenhalgh, S., and E. Manukyan, 2013, Seismic reflection for hardrock mineral exploration: Lessons from numerical modeling: Journal of Environmental & Engineering Geophysics, **18**, 281–296, doi: 10.2113/JEEG18.4.281.

Greenhalgh, S. A., I. M. Mason, E. Lucas, D. Pant, and R. T. Eames, 1990, Controlled direction reception filtering of P- and S-waves in P space: Geophysical Journal International, **100**, 221–234, doi: 10.1111/j.1365-246X.1990.tb02482.x.

Greenhalgh, S., B. Zhou, and S. Cao, 2003, A crosswell seismic experiment for nickel sulphide exploration: Journal of Applied Geophysics, **53**, 77–89, doi: 10.1016/S0926-9851(03)00029-6.

Green, A. G., and J. A. Mair, 1983, Subhorizontal fractures in a granitic pluton: Their detection and implications for radioactive waste disposal: Geophysics, **48**, 1428–1449, doi: 10.1190/1.1441428.

Hardage, B. A., 2000, Vertical seismic profiling: Principles (Handbook of geophysical exploration: Seismic exploration): Elsevier 14, 552.

Hardage, B. A., M. V. DeAngelo, P. E. Murray, and D. Sava, 2011, Multicomponent seismic technology: SEG.

Hicks, G. J., and R. G. Pratt, 2001, Reflection waveform inversion using local descent methods: Estimating attenuation and velocity over a gas-sand deposit: Geophysics, **66**, 598–612, doi: 10.1190/1.1444951.

Hitchings, V. H., and H. Potters, 2000, Production and geologic implications of the Natih 9-C, 3-D seismic survey: The Leading Edge, **19**, 1117–1124, doi: 10.1190/1.1438490.

Hloušek, F., O. Hellwig, and S. Buske, 2015a, Three-dimensional focused seismic imaging for geothermal exploration in crystalline rock near Schneeberg, Germany: Geophysical Prospecting, **63**, 999–1014, doi: 10.1111/1365-2478.12239.

Hloušek, F., O. Hellwig, and S. Buske, 2015b, Improved structural characterization of the Earth's crust at the German Continental Deep Drilling Site using advanced seismic imaging techniques: Focused imaging at KTB: Journal of Geophysical Research: Solid Earth, **120**, 6943–6959, doi: 10.1002/2015JB012330.

Husen, S., and E. Kissling, 2001, Local earthquake tomography between rays and waves: Fat ray tomography: Physics of the Earth and Planetary Interiors, **123**, 127–147, doi: 10.1016/S0031-9201(00)00206-5.

Jäger, R., J. Mann, G. Höcht, and P. Hubral, 2001, Common-reflection-surface stack: Image and attributes: Geophysics, **66**, 97–109, doi: 10.1190/1.1444927.

Jordi, C., C. Schmelzbach, and S. Greenhalgh, 2016, Frequency-dependent traveltime tomography using fat rays: Application to near-surface seismic imaging: Journal of Applied Geophysics, **131**, 202–213, doi: 10.1016/j.jappgeo.2016.06.002.

Juhlin, C., M. Friberg, H. P. Echtler, T. Hismatulin, A. Rybalka, A. G. Green, and J. Ansorge, 1998, Crustal structure of the Middle Urals: Results from the (ESRU) Europrobe seismic reflection profiling in the Urals experiments: Tectonics, **17**, 710–725.

Juhlin, C., and H. Palm, 2003, Experiences from shallow reflection seismics over granitic rocks in Sweden, *in* D. W. Eaton, B. Milkereit, and M. H. Salisbury, eds., Hardrock seismic exploration: SEG, 93–109.

Khaidukov, V., E. Landa, and T. J. Moser, 2004, Diffraction imaging by focusing-defocusing: An outlook on seismic superresolution: Geophysics, **69**, 1478–1490, doi: 10.1190/1.1836821.

Klokov, A., and S. Fomel, 2012, Separation and imaging of seismic diffractions using migrated dip-angle gathers: Geophysics, **77**, no. 6, S131–S143, doi: 10.1190/geo2012-0017.1.

Kuriyagawa, M., and N. Tenma, 1999, Development of hot dry rock technology at the Hijiori test site: Geothermics, **28**, 627–636, doi: 10.1016/S0375-6505(99)00033-4.

Landa, E., and S. Keydar, 1998, Seismic monitoring of diffraction images for detection of local heterogeneities: Geophysics, **63**, 1093–1100, doi: 10.1190/1.1444387.

Lanz, E., D. E. Boerner, H. Maurer, and A. Green, 1998, Landfill delineation and characterization using electrical, electromagnetic and magnetic methods: Journal of Environmental and Engineering Geophysics, **3**, 185–196, doi: 10.4133/JEEG3.4.185.

Lewis, C., T. L. Davis, and C. Vuillermoz, 1991, Three-dimensional multicomponent imaging of reservoir heterogeneity, Silo Field, Wyoming: Geophysics, **56**, 2048–2056, doi: 10.1190/1.1443017.

Li, X.-Y., and M. C. Mueller, 1997, Case studies of multicomponent seismic data for fracture characterization: Austin Chalk examples, *in* I. Palaz, and K. J. Marfurt, eds., Carbonate seismology: SEG, 337–372.

Lipman, S. C., C. J. Strobel, and M. S. Gulati, 1978, Reservoir performance of The Geysers Field: Geothermics, **7**, 209–219, doi: 10.1016/0375-6505(78)90011-1.

Lumley, D. E., 2001, Time-lapse seismic reservoir monitoring: Geophysics, **66**, 50–53, doi: 10.1190/1.1444921.

Lund, J. W., 2009, Characteristics, development and utilization of geothermal resources: Geo-Heat Centre Quarterly Bulletin, **28**, 1–9.

Luo, M., and B. J. Evans, 2004, An amplitude-based multi-azimuthal approach to mapping fractures using P-wave 3D seismic data: Geophysics, **69**, 690–698, doi: 10.1190/1.1759455.

Lüschen, E., S. Görne, H. von Hartmann, R. Thomas, and R. Schulz, 2015, 3D seismic survey for geothermal exploration in crystalline rocks in Saxony, Germany: 3D seismic survey for geothermal exploration: Geophysical Prospecting, **63**, 975–989, doi: 10.1111/1365-2478.12249.

Lüschen, E., M. Wolfgramm, T. Fritzer, M. Dussel, R. Thomas, and R. Schulz, 2014, 3D seismic survey explores geothermal targets for reservoir characterization at Unterhaching, Munich, Germany: Geothermics, **50**, 167–179, doi: 10.1016/j.geothermics.2013.09.007.

Majer, E. L., T. V. McEvilly, F. S. Eastwood, and L. R. Myer, 1988, Fracture detection using P-wave and S-wave vertical seismic profiling at The Geysers: Geophysics, **53**, 76–84, doi: 10.1190/1.1442401.

Malehmir, A., R. Durrheim, G. Bellefleur, M. Urosevic, C. Juhlin, D. J. White, B. Milkereit, and G. Campbell, 2012, Seismic methods in mineral exploration and mine planning: A general overview of past and present case histories and a look into the future: Geophysics, **77**, no. 5, WC173–WC190, doi: 10.1190/geo2012-0028.1.

Malehmir, A., C. Schmelzbach, E. Bongajum, G. Bellefleur, C. Juhlin, and A. Tryggvason, 2009, 3D constraints on a possible deep >2.5 km massive sulphide mineralization from 2D crooked-line seismic reflection data in the Kristineberg mining area, northern Sweden: Tectonophysics, **479**, 223–240.

Malinowski, M., S. Operto, and A. Ribodetti, 2011, High-resolution seismic attenuation imaging from wide-aperture onshore data by visco-acoustic frequency-domain full-waveform inversion: Attenuation imaging: Geophysical Journal International, **186**, 1179–1204, doi: 10.1111/j.1365-246X.2011.05098.x.

Manukyan, E., S. Latzel, H. Maurer, S. Marelli, and S. A. Greenhalgh, 2012, Exploitation of data-information content in elastic-waveform inversions: Geophysics, **77**, no. 2, R105–R115, doi: 10.1190/geo2011-0184.1.

Matsushima, J., and Y. Okubo, 2003, Rheological implications of the strong seismic reflector in the Kakkonda geothermal field, Japan: Tectonophysics, **371**, 141–152, doi: 10.1016/S0040-1951(03)00213-0.

Milkereit, B., and D. Eaton, 1998, Imaging and interpreting the shallow crystalline crust: Tectonophysics, **286**, 5–18.

Milkereit, B., A. Green, J. Wu, D. White, and E. Adam, 1994, Integrated seismic and borehole geophysical study of the Sudbury Igneous Complex: Geophysical Research Letters, **21**, 931–934, doi: 10.1029/93GL03424.

Moser, T. J., and C. B. Howard, 2008, Diffraction imaging in depth: Geophysical Prospecting, **56**, 627–641, doi: 10.1111/j.1365-2478.2007.00718.x.

Muñoz, G., 2014, Exploring for geothermal resources with electromagnetic methods: Surveys in Geophysics, **35**, 101–122, doi: 10.1007/s10712-013-9236-0.

Muñoz, G., K. Bauer, I. Moeck, A. Schulze, and O. Ritter, 2010, Exploring the Groß Schönebeck (Germany) geothermal site using a statistical joint interpretation of magnetotelluric and seismic tomography models: Geothermics, **39**, 35–45, doi: 10.1016/j.geothermics.2009.12.004.

Nakagome, O., T. Uchida, and T. Horikoshi, 1998, Seismic reflection and VSP in the Kakkonda geothermal field, Japan: Fractured reservoir characterization: Geothermics, **27**, 535–552, doi: 10.1016/S0375-6505(98)00032-7.

Obermann, A., T. Kraft, E. Larose, and S. Wiemer, 2015, Potential of ambient seismic noise techniques to monitor the St. Gallen geothermal site (Switzerland): Monitoring the St. Gallen geothermal site: Journal of Geophysical Research: Solid Earth, **120**, 4301–4316, doi: 10.1002/2014JB011817.

Operto, S., C. Ravaut, L. Improta, J. Virieux, A. Herrero, and P. Dell'Aversana, 2004, Quantitative imaging of complex structures from dense wide-aperture seismic data by multiscale traveltime and waveform inversions: A case study: Geophysical Prospecting, **52**, 625–651, doi: 10.1111/j.1365-2478.2004.00452.x.

Özbek, A., 2000, Multichannel adaptive interference cancelling: SEG, 2088–2091.

Place, J., M. Diraison, C. Naville, Y. Géraud, M. Schaming, and C. Dezayes, 2010, Decoupling of deformation in the Upper Rhine Graben sediments. Seismic reflection and diffraction on 3-component vertical seismic profiling (Soultz-sous-Forêts area): Comptes Rendus Geoscience, **342**, 575–586, doi: 10.1016/j.crte.2010.01.001.

Place, J., J. Sausse, J.-M. Marthelot, M. Diraison, Y. Géraud, and C. Naville, 2011, 3-D mapping of permeable structures affecting a deep granite basement using isotropic 3C VSP data: Mapping structures in a deep granite basement: Geophysical Journal International, **186**, 245–263, doi: 10.1111/j.1365-246X.2011.05012.x.

Pratt, R. G., 1999, Seismic waveform inversion in the frequency domain, Part 1: Theory and verification in a physical scale model: Geophysics, **64**, 888–901, doi: 10.1190/1.1444597.

Pratt, R. G., and N. R. Goulty, 1991, Combining wave-equation imaging with traveltime tomography to form high-resolution images from crosshole data: Geophysics, **56**, 208–224, doi: 10.1190/1.1443033.

Pratt, R. G., W. J. McGaughey, and C. H. Chapman, 1993, Anisotropic velocity tomography: A case study in a near-surface rock mass: Geophysics, **58**, 1748–1763, doi: 10.1190/1.1443389.

Pratt, R. G., and R. M. Shipp, 1999, Seismic waveform inversion in the frequency domain, Part 2: Fault delineation in sediments using crosshole data: Geophysics, **64**, 902–914, doi: 10.1190/1.1444598.

Pussak, M., K. Bauer, M. Stiller, and W. Bujakowski, 2014, Improved 3D seismic attribute mapping by CRS stacking

instead of NMO stacking: Application to a geothermal reservoir in the Polish Basin: Journal of Applied Geophysics, **103**, 186–198, doi: 10.1016/j.jappgeo.2014.01.020.
Rabbel, W., T. Beilecke, T. Bohlen, D. Fischer, A. Frank, J. Hasenclever, G. Borm, J. Kück, K. Bram, G. Druivenga, E. Lüschen, H. Gebrande, J. Pujol, and S. Smithson, 2004, Superdeep vertical seismic profiling at the KTB deep drill hole (Germany): Seismic close-up view of a major thrust zone down to 8.5 km depth: Journal of Geophysical Research, **109**, doi: 10.1029/2004JB002975.
Raknes, E. B., and B. Arntsen, 2015, A numerical study of 3D elastic time-lapse full-waveform inversion using multicomponent seismic data: Geophysics, **80**, no. 6, R303–R315, doi: 10.1190/geo2014-0472.1.
Raknes, E. B., B. Arntsen, and W. Weibull, 2015, Three-dimensional elastic full waveform inversion using seismic data from the Sleipner area: Geophysical Journal International, **202**, 1877–1894, doi: 10.1093/gji/ggv258.
Rawlinson, N., and M. Sambridge, 2003, Seismic traveltime tomography of the crust and lithosphere, *in* R. Dmowska, ed., Advances in geophysics: Elsevier, 81–198.
Reshetnikov, A., J. Kummerow, H. Asanuma, M. Häring, and S. A. Shapiro, 2015, Microseismic reflection imaging and its application to the Basel geothermal reservoir: Geophysics, **80**, no. 6, WC39–WC49, doi: 10.1190/geo2014-0593.1.
Rial, J. A., M. Elkibbi, and M. Yang, 2005, Shear-wave splitting as a tool for the characterization of geothermal fractured reservoirs: Lessons learned: Geothermics, **34**, 365–385, doi: 10.1016/j.geothermics.2005.03.001.
Richards, H. G., R. H. Parker, A. S. P. Green, R. H. Jones, J. D. M. Nicholls, D. A. C. Nicol, M. M. Randall, S. Richards, R. C. Stewart, and J. Willis-Richards, 1994, The performance and characteristics of the experimental hot dry rock geothermal reservoir at Rosemanowes, Cornwall (1985–1988): Geothermics, **23**, 73–109, doi: 10.1016/0375-6505(94)90032-9.
Riedel, M., C. Dutsch, C. Alexandrakis, I. Dini, S. Ciuffi, and S. Buske, 2015, Seismic depth imaging of a geothermal system in Southern Tuscany: Seismic depth imaging: Geophysical Prospecting, **63**, 957–974, doi: 10.1111/1365-2478.12254.
Robertsson, J. O. A., and J. O. Blanch, 2011, Numerical methods, finite difference, *in* H. K. Gupta, ed., Encyclopedia of solid earth geophysics: Springer Netherlands, 883–892.
Robertsson, J. O. A., K. Holliger, and A. G. Green, 1996, Source-generated noise in shallow seismic data: European Journal of Environmental Geophysics, **1**, 107–124.
Rutty, M. J., and S. A. Greenhalgh, 1993, The correlation of seismic events on multicomponent data in the presence of coherent noise: Geophysical Journal International, **113**, 343–358, doi: 10.1111/j.1365-246X.1993.tb00891.x.
Salisbury, M. W., C. W. Harvey, and L. Matthews, 2003, The acoustic properties of ores and host rocks in hardrock terranes, *in* D. W. Eaton, B. Milkereit, and M. H. Salisbury, eds., Hardrock seismic exploration: SEG, Geophysical Development Series, 9–19.
Sausse, J., C. Dezayes, L. Dorbath, A. Genter, and J. Place, 2010, 3D model of fracture zones at Soultz-sous-Forêts based on geological data, image logs, induced microseismicity and vertical seismic profiles: Comptes Rendus Geoscience, **342**, 531–545, doi: 10.1016/j.crte.2010.01.011.
Schellschmidt, R., B. Sanner, S. Pester, and R. Schulz, 2010, Geothermal energy use in Germany: Proceedings of the World Geothermal Congress.
Schmelzbach, C., H. Horstmeyer, and C. Juhlin, 2007, Shallow 3D seismic-reflection imaging of fracture zones in crystalline rock: Geophysics, **72**, no. 6, B149–B160, doi: 10.1190/1.2787336.
Schmelzbach, C., J. Kummerow, P. Wigger, A. Reshetnikov, P. Salazar, and S. A. Shapiro, 2016, Microseismic reflection imaging of the Central Andean crust: Geophysical Journal International, **204**, 1396–1404, doi: 10.1093/gji/ggv530.
Schmelzbach, C., J. F. Simancas, C. Juhlin, and R. Carbonell, 2008a, Seismic-reflection imaging over the South Portuguese Zone fold-and-thrust belt, SW Iberia: Journal of Geophysical Research, **113**, B08301, doi: 10.1029/2007JB005341.
Schmelzbach, C., C. A. Zelt, C. Juhlin, and R. Carbonell, 2008b, P and SV-velocity structure of the South Portuguese Zone fold-and-thrust belt, SW Iberia, from traveltime tomography: Geophysical Journal International, **175**, 689–712, doi: 10.1111/j.1365-246X.2008.03937.x.
Schön, J. H., 1996, Physical properties of rocks: Fundamentals and principles of petrophysics: Pergamon Press.
Schreiter, L., F. Hloušek, O. Hellwig, and S. Buske, 2015, Characterization of seismic reflections from faults in a crystalline environment, Schneeberg, Germany: Seismic reflections from faults: Geophysical Prospecting, **63**, 1015–1032, doi: 10.1111/1365-2478.12255.
Sheriff, R. E., and L. P. Geldart, 1995, Exploration seismology: Cambridge University Press.
Sirgue, L., O. I. Barkved, J. P. Van Gestel, O. J. Askim, and J. H. Kommedal, 2009, 3D waveform inversion on Valhall wide-azimuth OBC: EAGE.
Sirgue, L., and R. G. Pratt, 2004, Efficient waveform inversion and imaging: A strategy for selecting temporal frequencies: Geophysics, **69**, 231–248, doi: 10.1190/1.1649391.
Spetzler, J., Z. Xue, H. Saito, and O. Nishizawa, 2008, Case story: Time-lapse seismic crosswell monitoring of CO_2 injected in an onshore sandstone aquifer: Geophysical Journal International, **172**, 214–225, doi: 10.1111/j.1365-246X.2007.03614.x.
Stewart, R. R., J. E. Gaiser, R. J. Brown, and D. C. Lawton, 2002, Converted-wave seismic exploration: Methods: Geophysics, **67**, 1348–1363, doi: 10.1190/1.1512781.
Stewart, R. R., J. E. Gaiser, R. J. Brown, and D. C. Lawton, 2003, Converted-wave seismic exploration: Applications: Geophysics, **68**, 40–57, doi: 10.1190/1.1543193.
Symes, W. W., 2008, Migration velocity analysis and waveform inversion: Geophysical Prospecting, **56**, 765–790, doi: 10.1111/j.1365-2478.2008.00698.x.

Taner, M. T., 2001, Seismic attributes: CSEG Recorder, **26**, 49–56.
Taner, M. T., F. Koehler, and R. E. Sheriff, 1979, Complex seismic trace analysis: Geophysics, **44**, 1041–1063, doi: 10.1190/1.1440994.
Taner, M. T., J. S. Schuelke, R. O'Doherty, and E. Baysal, 1994, Seismic attributes revisited: SEG, 1104–1106.
Tang, C., J. A. Rial, and J. M. Lees, 2008, Seismic imaging of the geothermal field at Krafla, Iceland using shear-wave splitting: Journal of Volcanology and Geothermal Research, **176**, 315–324, doi: 10.1016/j.jvolgeores.2008.04.017.
Tarantola, A., 1984, Inversion of seismic reflection data in the acoustic approximation: Geophysics, **49**, 1259–1266, doi: 10.1190/1.1441754.
Tatham, R. H., and M. D. McCormack, 1991, Multicomponent seismology in petroleum exploration: SEG, SEG Investigations in Geophysics Series 6.
Tester, J. W., B. J. Anderson, A. S. Batchelor, D. D. Blackwell, R. DiPippo, E. M. Drake, J. Garnish, B. Livesay, M. C. Moore, K. Nichols, S. Petty, M. N. Toksoz, R. W. Veatch, R. Baria, C. Augustine, E. Murphy, P. Negraru, and M. Richards, 2007, Impact of enhanced geothermal systems on US energy supply in the twenty-first century: Philosophical Transactions. Series A, Mathematical, Physical, and Engineering Sciences, **365**, 1057–1094, doi: 10.1098/rsta.2006.1964.
Thomas, R., E. Lüschen, and R. Schulz, 2010, Seismic reflection exploration of Karst phenomena of a geothermal reservoir in Southern Germany: Proceedings of the World Geothermal Congress.
Thomas, R., and R. Schulz, 2007, Facies differentiation of the Malm by interpretation of reflection seismic profiles and a moving source VSP Experiment: Proceedings of the European Geothermal Congress.
Tsvankin, I., 2012, Seismic signatures and analysis of reflection data in anisotropic media, 3rd ed.: SEG.
Vasco, D. W., J. E. Peterson, and E. L. Majer, 1995, Beyond ray tomography: Wavepaths and Fresnel volumes: Geophysics, **60**, 1790–1804, doi: 10.1190/1.1443912.
Vécsey, G., K. Holliger, R. G. Pratt, B. C. Dyer, and A. G. Green, 1998, Anisotropic seismic tomography of a potential hot dry rock reservoir before and during induced pressurization: Geophysical Research Letters, **25**, 1991–1994, doi: 10.1029/98GL01414.
Vidale, J. E., 1986, Complex polarization analysis of particle motion: Bulletin of the Seismological Society of America, **76**, 1393–1405.
Vigh, D., K. Jiao, D. Watts, and D. Sun, 2014, Elastic full-waveform inversion application using multicomponent measurements of seismic data collection: Geophysics, **79**, no. 2, R63–R77, doi: 10.1190/geo2013-0055.1.
Virieux, J., and S. Operto, 2009, An overview of full-waveform inversion in exploration geophysics: Geophysics, **74**, no. 6, WCC1–WCC26, doi: 10.1190/1.3238367.
von Hartmann, H., H. Buness, C. M. Krawczyk, and R. Schulz, 2012, 3-D seismic analysis of a carbonate platform in the Molasse Basin — Reef distribution and internal separation with seismic attributes: Tectonophysics, **572–573**, 16–25, doi: 10.1016/j.tecto.2012.06.033.
Weber, J., B. Ganz, R. Schellschmidt, B. Sanner, and R. Schulz, 2015, Geothermal energy use in Germany: Proceedings of the World Geothermal Congress.
Wei, S., M. V. DeAngelo, and B. A. Hardage, 2014a, Advantages of joint interpretation of P-P and P-SV seismic data in geothermal exploration: Interpretation, **2**, no. 2, SE117–SE123, doi: 10.1190/INT-2013-0084.1.
Wei, S., M. V. DeAngelo, and B. A. Hardage, 2014b, Interpretation of multicomponent seismic data across Wister geothermal field, Imperial Valley, California: Interpretation, **2**, no. 2, SE125–SE135, doi: 10.1190/INT-2013-0083.1.
Weijermars, R., G. Drijkoningen, T. J. Heimovaara, E. S. J. Rudolph, G. J. Weltje, and K. H. A. A. Wolf, 2011, Unconventional gas research initiative for clean energy transition in Europe: Journal of Natural Gas Science and Engineering, **3**, 402–412, doi: 10.1016/j.jngse.2011.04.002.
Woodward, M. J., 1992, Wave-equation tomography: Geophysics, **57**, 15–26, doi: 10.1190/1.1443179.
Yardley, G. S., and S. Crampin, 1991, Extensive-dilatancy anisotropy: Relative information in VSPs and reflection surveys: Geophysical Prospecting, **39**, 337–355, doi: 10.1111/j.1365-2478.1991.tb00316.x.
Yilmaz, Ö., 2001, Seismic data analysis. Processing, inversion, and interpretation of seismic data: SEG.
Zelt, C. A., and P. J. Barton, 1998, Three-dimensional seismic refraction tomography: A comparison of two methods applied to data from the Faeroe Basin: Journal of Geophysical Research, **103**, 7187–7210, doi: 10.1029/97JB03536.
Zhe, J., and S. A. Greenhalgh, 1997, Prestack multicomponent migration: Geophysics, **62**, 598–613, doi: 10.1190/1.1444169.
Zhou, B., S. Greenhalgh, and A. Green, 2008, Nonlinear traveltime inversion scheme for crosshole seismic tomography in tilted transversely isotropic media: Geophysics, **73**, no. 4, D17–D33, doi: 10.1190/1.2910827.

Biographies and photographs of the authors are not available.